

Characterization of collective excitations in weakly coupled disordered superconductorsBo Fan,^{1,*} Abhisek Samanta,^{2,†} and Antonio M. García-García^{1,‡}¹*Shanghai Center for Complex Physics, School of Physics and Astronomy, Shanghai Jiao Tong University, Shanghai 200240, China*²*Physics Department, Technion, Haifa 32000, Israel*

(Received 12 July 2021; revised 20 December 2021; accepted 9 March 2022; published 28 March 2022)

Isolated islands in two-dimensional strongly disordered and strongly coupled superconductors become optically active, inducing subgap collective excitations in the ac conductivity. Here, we investigate the fate of these excitations as a function of the disorder strength in the experimentally relevant case of weak electron-phonon coupling. An explicit calculation of the ac conductivity, that includes vertex corrections to restore gauge symmetry, reveals the existence of collective subgap excitations, related to phase fluctuations and therefore identified as the Goldstone modes, for intermediate to strong disorder. As disorder increases, the shape of the subgap excitation transits from peaked close to the spectral gap to a broader distribution reaching much smaller frequencies. Phase coherence still holds in part of this disorder regime. The requirement to observe subgap excitations is not the existence of isolated islands acting as nanoantennas but rather the combination of a sufficiently inhomogeneous order parameter with a phase fluctuation correlation length smaller than the system size. Our results indicate that, by tuning disorder, the Goldstone mode may be observed experimentally in metallic superconductors based, for instance, on Al, Sn, Pb, or Nb.

DOI: [10.1103/PhysRevB.105.094515](https://doi.org/10.1103/PhysRevB.105.094515)**I. INTRODUCTION**

Anderson stated [1] that the Bardeen-Cooper-Schrieffer (BCS) theory of superconductivity [2] had been the scientific love of his life. It is likely that collective modes were an important part of this love story. Shortly after the microscopic BCS theory [2] was proposed, Anderson [3,4] noticed that two of its most salient features, the existence of a gapped ground state and phase rigidity, were to some extent contradictory. If the phase of the order parameter were rigid, the $U(1)$ gauge symmetry is spontaneously broken. According to Goldstone's theorem [5,6], the spontaneous breaking of this $U(1)$ symmetry is associated to the existence of a zero-energy (massless) collective excitation, the so-called Goldstone mode. In principle, this is in apparent contradiction with the BCS prediction of a gapped ground state. However, Anderson argued [3] that for clean superconductors, later [7] shown to also hold for weakly disordered superconductors, the Goldstone mode is not observable because long-range Coulomb interactions shift its natural frequency to the plasmon frequency which is typically much higher than the spectroscopic gap.

Therefore, it came as a relative surprise that recent numerical results for the conductivity of two-dimensional strongly disordered and strongly coupled superconductors [8–15] have shown the existence of collective excitations below the spectral gap. The absorption of the incoming electromagnetic radiation occurs [8] in disorder-induced isolated superconducting islands that act as nanoantennas. The combination of strong disorder and strong coupling mixes zero and finite momentum modes so that collective modes contribute to the

optical response even in the long-wavelength limit. Moreover, it was argued [7,8] that long-range Coulomb interactions do not change this conclusion qualitatively. Although these [8] numerical results provide rather conclusive evidence on the existence of subgap collective excitations, they were obtained in the strong-coupling limit, which is not strictly applicable in most metallic superconductors such as Sn, Nb, Al, or Pb whose electron-phonon coupling is weak or intermediate. We note that the combined effect of phase and amplitude fluctuations was investigated in detail in Ref. [16] by quantum Monte Carlo techniques, though the focus was on the evolution of the gap across the superconductor-insulator transition at both zero and finite temperature rather than collective excitation and transport properties.

On the experimental front, there are also recent observations of a subgap structure in the optical conductivity of several disordered weakly coupled superconductors [12,17–20] (see also Refs. [21–30] for related developments). In NbN and InO [12,31] close to the superconductor-insulator transition, subgap weight has been related to amplitude fluctuations, the Higgs mode [32]. In granular aluminum [33], the observation of spectral weight below the gap at a relatively high temperature was associated with the Goldstone mode, though the agreement with the theoretical predictions was only qualitative. Another experiment [34] involving granular aluminum, performed at lower temperatures, reported a broad subgap peak whose origin remains unexplained. The conclusion is that, despite promising advances, there is no conclusive evidence yet that the different subgap excitations observed experimentally are the sought Goldstone and Higgs modes due to both the qualitative nature of the theoretical predictions and the difficulty in ruling out other experimental causes, such as the effect of the substrate or competing quantum orders.

*bo.fan@sjtu.edu.cn

†abhiseks@campus.technion.ac.il

‡amgg@sjtu.edu.cn

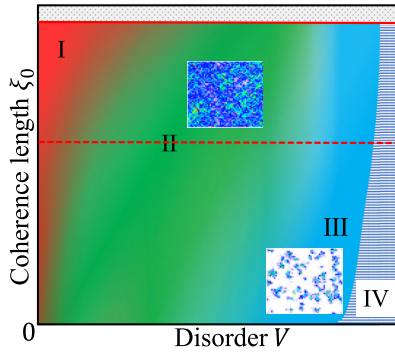


FIG. 1. Summary of the subgap optical conductivity as a function of disorder V and the electron-phonon coupling strength parametrized by the clean coherence length ξ_0 . I (red): Region of very weak disorder where no collective excitations are expected either due to Coulomb interactions or because the collective mode is still gapless. II (green): Collective excitations can be observed and only require a sufficiently inhomogeneous order parameter. We illustrate it with a miniplot of the site dependence of the order parameter for $U = 1$, $V = 1.5$. The dashed red line separates the weak-coupling (above) and strong-coupling (below) regions. Numerically, we explore the range $\xi_0 \lesssim 500$ nm that includes most weakly coupled metallic superconductors (above the dashed line). III (blue): Collective excitations are related to isolated superconducting islands. Here, the miniplot is for $U = 5$, $V = 3$. The strong-coupling limit was previously studied in Ref. [8]. IV: Anderson insulator region. The top gray dotted region $\xi_0 \rightarrow \infty$ is not accessible numerically. The employed color code aims only to differentiate the different regions. It is not related to the value of any observable.

In this paper, we investigate collective excitations in a fermionic model of two-dimensional disordered superconductors focusing on the optical response captured by the low-frequency ac conductivity. Our analysis is based on the Bogoliubov–de Gennes (BdG) mean-field formalism which leads to the so-called *bare bubble* diagram in the calculation of the conductivity, plus its vertex corrections [35] which include fluctuations around the mean-field order parameter (namely amplitude, phase, and density fluctuations) evaluated within the random phase approximation [3,36]. This is the minimal calculation scheme that restores gauge invariance and therefore can describe collective excitations. We reach a maximum size of $L = 30$ while the maximum size in previous works was $L = 20$ [8,9]. This allows us to explore the weak-coupling limit. Since we show that already for $L = 26$ finite size effects are not important, results in the paper are mostly restricted to this size.

In Fig. 1, we sketch the pattern of subgap excitations in the ac conductivity as a function of the strength of disorder and electron-phonon coupling. The main results of the paper correspond to region II (green), especially above the dashed red line, where we identify the Goldstone mode in weakly coupled superconductors whose detectability only requires a sufficiently inhomogeneous [37–45] order parameter. Region III (blue) corresponds to the region where the subgap optical response is related to isolated islands [8]. The strong-coupling region was previously studied in Ref. [8].

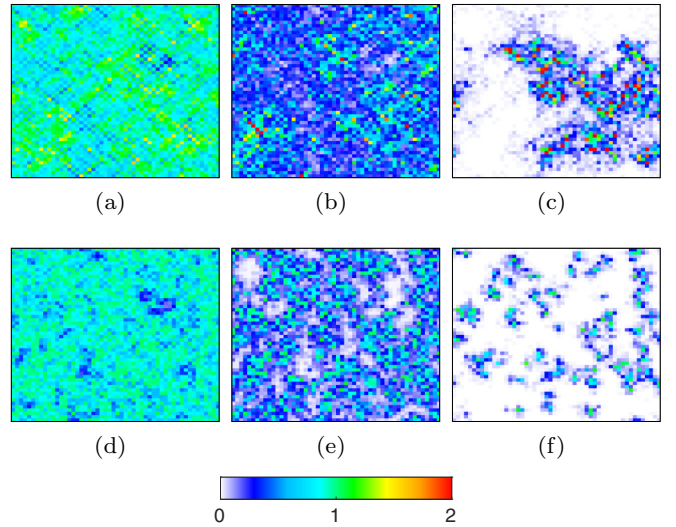


FIG. 2. Amplitude of the order parameter $\Delta(r_i)$ resulting from the solution of the BdG equations, normalized by its value Δ_0 in the clean limit. The spatial maps are plotted on a square lattice of size $N = 52 \times 52$, with $\langle n \rangle = 0.875$. Upper: $U = 1$. Lower: $U = 5$. Disorder strength, from left to right, is $V = 0.5, 1.5$, and 3 .

II. THEORETICAL FORMALISM

We initiate our analysis with a brief summary of the employed theoretical framework leading to the calculation of the ac conductivity (see Supplemental Material [36] for details). We start from the two-dimensional Bogoliubov–de Gennes equations [38,39,46,47] in the presence of a uniformly distributed random potential $V_i \in [-V, V]$ and an electron-phonon coupling U ,

$$\begin{pmatrix} \hat{K} & \hat{\Delta} \\ \hat{\Delta}^* & -\hat{K}^* \end{pmatrix} \begin{pmatrix} u_n(i) \\ v_n(i) \end{pmatrix} = E_n \begin{pmatrix} u_n(i) \\ v_n(i) \end{pmatrix}, \quad (1)$$

where $\hat{K}u_n(i) = -t \sum_{\delta} u_n(i + \delta) + (V_i - \mu_i)u_n(i)$, in which δ means the four nearest-neighboring sites, and $\mu_i = \mu + Uu_n(i)/2$ is the chemical potential that incorporates a site-dependent Hartree shift. The BdG equations are completed by self-consistency conditions for the site-dependent order parameter amplitude $\Delta(i) = U \sum_n u_n(i)v_n^*(i)$ and the density $n(i) = 2 \sum_n |v_n(i)|^2$, that are also outputs of the numerical calculation. All the presented results are for a square lattice ($N = L \times L$) with periodic or Dirichlet boundary conditions. We fix the averaged density $\langle n \rangle = \sum_i n(i)/N$ and let the chemical potential μ vary. As an example of the BdG solution, that illustrates the differences between weak $U = 1$ and strong $U = 5$ coupling, in Fig. 2, we depict $\Delta(i)$ in these two regimes. For strong disorder, the order parameter is distributed in small islands, while for weak coupling we observe an intricate, highly inhomogeneous spatial structure with no visible islands. This stark difference will be important in the following analysis of the conductivity.

The second step of the calculation is the evaluation of the response function [8], $\chi_{ij}(j^x, j^x) = -i \int dt e^{i\omega t} \langle [j_i^x(t), j_j^x(0)] \rangle$ in the presence of fluctuations of the order parameter, amplitude A_i and phase Φ_i , and density δn_i where j^x stands for the current along the x

direction and i, j are site indices. These corrections to the BdG results, evaluated using the random phase approximation [8,36], that includes vertex corrections required to restore gauge invariance, leads to

$$\chi_{ij}(j^x, j^x) = \chi_{ij}^0(j^x, j^x) + \Lambda_{ip} \mathbb{V}_{pl} (\mathbb{I}_{3N \times 3N} - \chi^B \mathbb{V})_{ls}^{-1} \bar{\Lambda}_{sj}. \quad (2)$$

Here, χ^0 is the bare current-current correlation function, Λ is the correlation function between current and one of the fluctuation components, χ^B is the bare mean-field susceptibility, and \mathbb{V} is the effective local interaction, defined by a 3×3 matrix in the fluctuation basis. Importantly, all these quantities [36] can be expressed in terms of the parameters of the model and the output of the previous BdG calculation. Before we embark in the calculation of the conductivity, we aim to characterize collective excitations by investigating the spatial structure of these susceptibilities, $C^{ab}(r, \omega) = \langle \tilde{\chi}^{ab}(r, \omega) \rangle / \langle \tilde{\chi}^{ab}(0, \omega) \rangle$, where $r = |r_i - r_j|$, $\langle \dots \rangle$ stands for spatial and disorder average, a, b label the fluctuation channel, $\tilde{\chi}^{ab}$ is the block matrix of $\tilde{\chi}^B$ (see Supplemental Material [36] for details), and

$$\tilde{\chi}^B = (\mathbb{I}_{3N \times 3N} - \chi^B \mathbb{V})^{-1} \chi^B. \quad (3)$$

In order to facilitate the interpretation and derivation of Eqs. (2) and (3), we provide an explicit representation of the Feynman's diagrams leading to these expressions in the Supplemental Material [36]. In the weak-coupling limit, we shall see that in most cases, subgap weight in the conductivity is dominated by phase fluctuations $a = b = \Phi$, so we restrict to this channel,

$$C(r, \omega) \equiv C^{\Phi\Phi}(r, \omega). \quad (4)$$

Physically, it describes phase correlations in points of the sample separated by a distance r after a perturbation of energy ω . If $C(r, \omega) > 0$ for $r \rightarrow \infty$, phase coherence holds. For our purposes, we define a *dephasing* length ℓ as the typical distance between a local maximum and a local minimum in $C(r, \omega)$. A necessary condition for the existence of phase collective excitations, the Goldstone mode, at a given energy ω , is that $\ell < L$, otherwise phases are not sufficiently uncorrelated to become optically active. For clean or weak disorder, and a small $\omega \ll$ two-particle spectral gap (ω_g), $C(r, \omega) \geq 0$ decays monotonously so phase fluctuations are still too correlated for a Goldstone mode to be observed. For very strong disorder, $C(r, \omega) \rightarrow 0$ quickly so no collective excitations can occur. For intermediate disorder, we expect that phases become sufficiently uncorrelated but still phase coherence can hold. This behavior is naturally related to oscillations in $C(r, \omega)$ that can become negative, signaling phase fluctuations are strong enough that phases in distant points become anticorrelated. Qualitatively, the number of optically active regions is given by the number of times that $C(r, \omega)$ switches sign (see Supplemental Material [36] for more details). If these features occur for $\omega < \omega_g$, the Goldstone mode is observed as a subgap excitation of the ac conductivity.

Numerical results largely confirm this picture. In the clean or weak disorder region $V \leq 0.5$ [Figs. 3(a) and 3(b)], oscillations around 0 only occur in a narrow window of energies above ω_g ($\omega \sim \omega_g$ when $V = 0.5$) and therefore are not

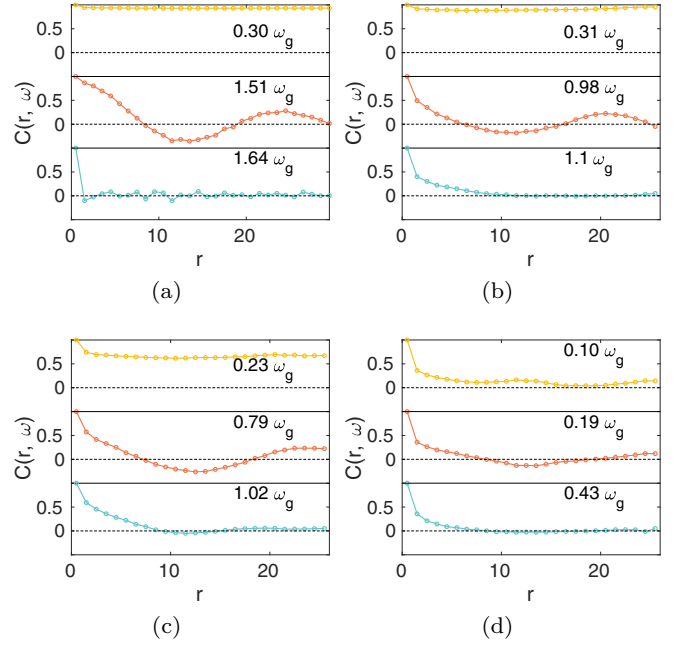


FIG. 3. $C(r, \omega)$ [Eq. (4)] for different ω in units of the two-particle spectral gap ω_g , $U = 1$, $L = 26$ (except for $V = 0$), $\langle n \rangle = 0.875$, and (a) $V = 0$ ($L = 30$), (b) $V = 0.5$, (c) $V = 1.5$, and (d) $V = 3.0$. The observed oscillations, with $C(r, \omega)$ alternating sign, is a defining feature of collective modes.

relevant for the observation of the Goldstone mode in the conductivity that requires a well-formed subgap peak. Phase coherence [$C(r, \omega) > 0$ for $r = L$] holds unless ω is not too large.

For sufficiently strong disorder $V = 1.5$ [Fig. 3(c)], and small ω , $C(r, \omega)$ decays rapidly to a constant positive value that indicates no optical activity. As ω approaches ω_g from below, we observe a much slower decay to a negative value, that defines the dephasing length ℓ , and indicates the presence of the subgap Goldstone mode. For even stronger disorder $V = 3$ [Fig. 3(d)], already in the insulating region, we observe similar features around $\omega \sim 0.2\omega_g$, inducing a negative value in $C(r, \omega)$.

III. GOLDSTONE MODE IN THE AC CONDUCTIVITY

In order to find out whether these modes are measurable, we now turn to the calculation of the ac conductivity. The real part of the optical conductivity is closely related [8–10] to the susceptibility computed previously,

$$\sigma(\omega) = \pi D_s \delta(\omega) + e^2 \text{Im} \frac{\chi(\omega)}{\omega}, \quad (5)$$

where Im stands for the imaginary part of $\chi(\omega) = 1/N \sum_{ij} \chi_{ij}(j^x, j^x)$, e is the elementary charge, $D_s = e^2 [\langle -k_x \rangle + \text{Re} \chi(\omega = 0)]$ is the superfluid stiffness, and $\langle -k_x \rangle = 4 \langle \sum_{n,i} v_n(i) v_n(i + \hat{x}) \rangle / N$ is the kinetic energy along the x direction. In Fig. 4, we depict the conductivity in the weak-coupling region $U = 1$ for different disorder strengths V . For $\langle n \rangle = 0.4$ and 0.6 , size effects could be important when $V \leq 1$, so for $V = 0.5$ we restrict ourselves to $\langle n \rangle = 0.875$ [see the inset of Fig. 4(a)], where this problem does

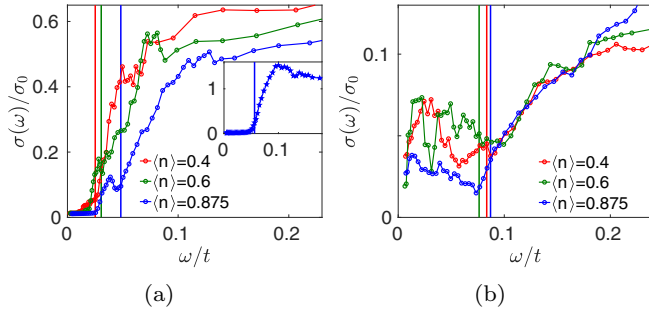


FIG. 4. Optical conductivity $\sigma(\omega)$ in units of $\sigma_0 = \frac{e^2}{h}$ for $U = 1$, $L = 26$ and different V and $\langle n \rangle$. Left: (a) $V = 1.5$, where the subgap excitation (Goldstone mode) starts to be observed. Inset: $U = 1$, $\langle n \rangle = 0.875$, $V = 0.5$. No subgap collective excitation. Right: (b) $V = 3$, the subgap spectral weight broadens, reaching very low frequencies.

not arise. Results are consistent with the previous calculation of $C(r, \omega)$. For weak disorder, we do not observe any clear subgap structure despite the fact that for $V \sim 1$ the order parameter is already strongly inhomogeneous. This is in contrast with the strong-coupling limit [8,36] where a subgap spectral weight is observed even for $V < 1$. Superficially, this seems surprising because strong coupling means a much larger order parameter. However, note that the existence of collective excitations depends on how correlated in space is the order parameter. In weakly coupled superconductors, due to a larger coherence length, neighboring sites are more likely to be correlated, which makes them more difficult to become optically active.

We do observe a clear subgap weight related to collective excitations only for $V \gtrsim 1.5$. For $V \sim 1.5$, the subgap mode is peaked close to ω_g with no spectral weight elsewhere, also in agreement with $C(r, \omega)$ [see Fig. 3(c)]. This indicates that only one or very few large domains become optically active. As V increases, the typical length ℓ that controls the decay of $C(r, \omega)$ becomes smaller and more domains become optically active, resulting in a broader spectrum [see Fig. 4(b) for $V = 3$]. The region $V > 3$ (not shown) is similar to the disordered strong-coupling limit where no phase coherence holds and only isolated islands act as nanoantennas for the partial absorption of the electromagnetic radiation. As a further confirmation of the relation between collective excitations and the existence of a *dephasing* length ℓ , not related to isolated islands, we compute the conductivity for different sizes L using Dirichlet boundary conditions that enhance finite-size effects as it is imposed that the order parameter vanishes at the boundary. The idea is that for a given disorder strength, we will observe collective excitations around ω_g only if $\ell < L$. For smaller sizes, phases are not sufficiently uncorrelated for collective excitations to occur below ω_g . Results depicted in Figs. 5(b) and 5(c) confirm that for not too large V , a subgap peak requires a minimum system size. Moreover, $\sigma(\omega)$ and $C(r, \omega)$ [see Fig. 5(a)] are not qualitatively altered by the change in boundary conditions but, as was expected, finite-size effects are enhanced so the minimum disorder $V \sim 0.5$ at which collective excitation occurs is weaker than for periodic boundary conditions $V \sim 1.5$. This could help the experimen-

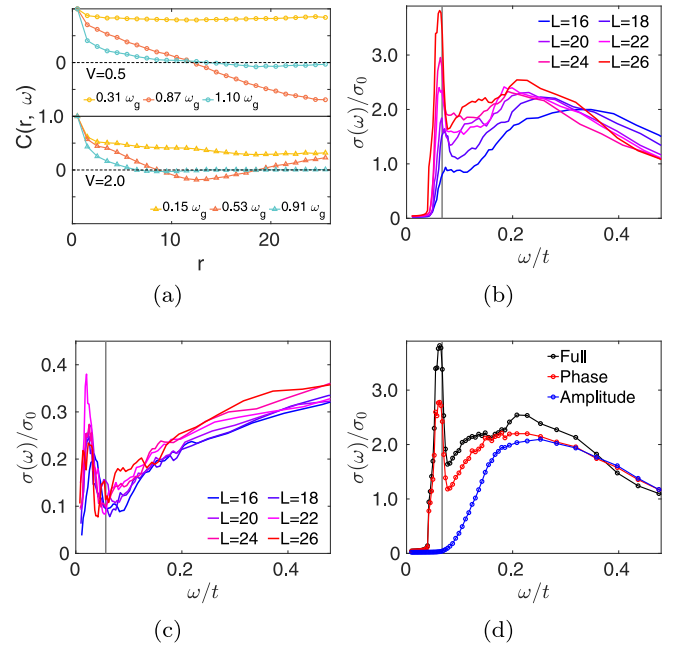


FIG. 5. Conductivity and $C(r, \omega)$ [Eq. (4)] for Dirichlet boundary conditions. (a) $C(r, \omega)$ for $U = 1$, $L = 26$, $\langle n \rangle = 0.875$. Upper: $V = 0.5$. Lower: $V = 2.0$. (b) $\sigma(\omega)$ for different sizes L , with parameters of (d). We observe a subgap collective excitation only for $L \geq 18$. This is the typical length ℓ for some substantial dephasing to occur so that the region becomes optically active. (c) $\sigma(\omega)$ for different sizes L , with parameters of (a). We observe subgap spectral weight at similar energies for all sizes. This is fully consistent with $C(r, \omega)$ in (a). (d) $\sigma(\omega)$ for $U = 1$, $V = 0.5$, $L = 26$, and $\langle n \rangle = 0.875$. Phase fluctuations control the subgap weight which is interpreted as the Goldstone mode.

tal observation of collective excitations in submicron flakes [43] of disordered superconductors.

We have referred to the subgap spectral weight as the Goldstone mode in several occasions but, so far, we have not provided explicit evidence that this is the case. This is remedied in Fig. 5(d), where it is shown that the conductivity, including full vertex corrections and still using Dirichlet boundary conditions, is qualitatively similar if only phase fluctuations are considered.

IV. RELATION TO EXPERIMENTS

For the experimental confirmation of these results, it is important that the explored parameters $U = 1$, $\langle n \rangle = 0.4, 0.6$, and 0.875 describe weakly coupled materials such as Al, Sn, Pb, or Nb. A simple calculation of the coherence length ξ_0 based on Δ_0 , and standard BCS relations, yields that our results apply to materials with $\xi_0 \lesssim 500$ nm which, though short for Al, cover most weakly coupled materials. We stress that in the relevant $V \geq 1$ region, finite-size effects for all $\langle n \rangle$ are negligible. Another important issue is whether the Coulomb interactions, neglected here, alter qualitatively our main findings. In Ref. [8] it was argued that, at least for the conductivity, this is not the case. We also believe that, at least for not very strong disorder, the long-range Coulomb interaction is heavily suppressed and therefore it should not alter

substantially the Goldstone mode typical frequency. It is an open question to what extent other features are quantitatively influenced by residual Coulomb interactions.

V. CONCLUSIONS

In summary, we have shown that subgap excitations in the optical conductivity can be observed in weakly coupled disordered superconductors provided that spatial inhomogeneities of the order parameter are sufficiently strong so that the typical length of decay of phase fluctuations is smaller than the system size. Therefore, unlike strongly coupled superconductors [8], collective excitations can coexist with a finite supercurrent and do not require the existence of isolated superconducting

islands acting as nanoantennas. We expect our results will stimulate experimental interest in this problem that could lead to a full characterization of collective modes in disordered metallic superconductors.

ACKNOWLEDGMENTS

B.F. and A.M.G.G. acknowledge financial support from a Shanghai talent program, from the National Natural Science Foundation China (NSFC) (Grant No. 11874259) and from the National Key R&D Program of China (Project ID 2019YFA0308603). A.M.G.G. is thankful for valuable conversations with Lara Benfatto. A.S. and B.F. are thankful for illuminating conversations with Goetz Seibold that, among other things, helped solve a technical problem with the code.

-
- [1] L. N. Cooper and D. Feldman, *BCS: 50 Years* (World Scientific, Singapore, 2010), Chap. 8.
- [2] J. Bardeen, L. N. Cooper, and J. R. Schrieffer, Theory of superconductivity, *Phys. Rev.* **108**, 1175 (1957).
- [3] P. W. Anderson, Random-Phase Approximation in the Theory of Superconductivity, *Phys. Rev.* **112**, 1900 (1958).
- [4] P. W. Anderson, Plasmons, gauge invariance, and mass, *Phys. Rev.* **130**, 439 (1963).
- [5] Y. Nambu, Quasi-particles and gauge invariance in the theory of superconductivity, *Phys. Rev.* **117**, 648 (1960).
- [6] J. Goldstone, Field theories with “superconductor” solutions, *Nuovo Cimento* **19**, 154 (1961).
- [7] D. Belitz, S. De Souza-Machado, T. P. Devereaux, and D. W. Hoard, Electromagnetic response of disordered superconductors, *Phys. Rev. B* **39**, 2072 (1989).
- [8] T. Cea, D. Bucheli, G. Seibold, L. Benfatto, J. Lorenzana, and C. Castellani, Optical excitation of phase modes in strongly disordered superconductors, *Phys. Rev. B* **89**, 174506 (2014).
- [9] T. Cea, C. Castellani, G. Seibold, and L. Benfatto, Non-relativistic Dynamics of the Amplitude (Higgs) Mode in Superconductors, *Phys. Rev. Lett.* **115**, 157002 (2015).
- [10] G. Seibold, L. Benfatto, C. Castellani, and J. Lorenzana, Amplitude, density, and current correlations of strongly disordered superconductors, *Phys. Rev. B* **92**, 064512 (2015).
- [11] S. V. Barabash and D. Stroud, Models for enhanced absorption in inhomogeneous superconductors, *Phys. Rev. B* **67**, 144506 (2003).
- [12] D. Sherman, U. S. Pracht, B. Gorshunov, S. Poran, J. Jesudasan, M. Chand, P. Raychaudhuri, M. Swanson, N. Trivedi, A. Auerbach *et al.*, The Higgs mode in disordered superconductors close to a quantum phase transition, *Nat. Phys.* **11**, 1882 (2015).
- [13] M. Swanson, Y. L. Loh, M. Randeria, and N. Trivedi, Dynamical Conductivity across the Disorder-Tuned Superconductor-Insulator Transition, *Phys. Rev. X* **4**, 021007 (2014).
- [14] G. Seibold, L. Benfatto, and C. Castellani, Application of the Mattis-Bardeen theory in strongly disordered superconductors, *Phys. Rev. B* **96**, 144507 (2017).
- [15] A. Samanta, A. Ratnakar, N. Trivedi, and R. Sensarma, Two-particle spectral function for disordered *s*-wave superconductors: Local maps and collective modes, *Phys. Rev. B* **101**, 024507 (2020).
- [16] K. Bouadim, Y. L. Loh, M. Randeria, and N. Trivedi, Single- and two-particle energy gaps across the disorder-driven superconductor-insulator transition, *Nat. Phys.* **7**, 884 (2011).
- [17] R. W. Crane, N. P. Armitage, A. Johansson, G. Sambandamurthy, D. Shahar, and G. Grüner, Fluctuations, dissipation, and nonuniversal superfluid jumps in two-dimensional superconductors, *Phys. Rev. B* **75**, 094506 (2007).
- [18] E. F. C. Driessen, P. C. J. J. Coumou, R. R. Tromp, P. J. de Visser, and T. M. Klapwijk, Strongly Disordered TiN and NbTiN *s*-Wave Superconductors Probed by Microwave Electrodynamics, *Phys. Rev. Lett.* **109**, 107003 (2012).
- [19] M. Žemlička, P. Neilinger, M. Trgala, M. Rehák, D. Manca, M. Grajcar, P. Szabó, P. Samuely, S. Gaži, U. Hübner, V. M. Vinokur, and E. Il’ichev, Finite quasiparticle lifetime in disordered superconductors, *Phys. Rev. B* **92**, 224506 (2015).
- [20] U. S. Pracht, N. Bachar, L. Benfatto, G. Deutscher, E. Farber, M. Dressel, and M. Scheffler, Enhanced Cooper pairing versus suppressed phase coherence shaping the superconducting dome in coupled aluminum nanograins, *Phys. Rev. B* **93**, 100503(R) (2016).
- [21] M. Mondal, A. Kamlapure, M. Chand, G. Saraswat, S. Kumar, J. Jesudasan, L. Benfatto, V. Tripathi, and P. Raychaudhuri, Phase Fluctuations in a Strongly Disordered *s*-Wave NbN Superconductor Close to the Metal-Insulator Transition, *Phys. Rev. Lett.* **106**, 047001 (2011).
- [22] M. Chand, G. Saraswat, A. Kamlapure, M. Mondal, S. Kumar, J. Jesudasan, V. Bagwe, L. Benfatto, V. Tripathi, and P. Raychaudhuri, Phase diagram of the strongly disordered *s*-wave superconductor NbN close to the metal-insulator transition, *Phys. Rev. B* **85**, 014508 (2012).
- [23] M. Mondal, A. Kamlapure, S. C. Ganguli, J. Jesudasan, V. Bagwe, L. Benfatto, and P. Raychaudhuri, Enhancement of the finite-frequency superfluid response in the pseudogap regime of strongly disordered superconducting films, *Sci. Rep.* **3**, 1357 (2013).
- [24] B. Cheng, L. Wu, N. J. Laurita, H. Singh, M. Chand, P. Raychaudhuri, and N. P. Armitage, Anomalous gap-edge

- dissipation in disordered superconductors on the brink of localization, *Phys. Rev. B* **93**, 180511(R) (2016).
- [25] B. G. Orr, H. M. Jaeger, and A. M. Goldman, Local superconductivity in ultrathin Sn films, *Phys. Rev. B* **32**, 7586 (1985).
- [26] H. M. Jaeger, D. B. Haviland, B. G. Orr, and A. M. Goldman, Onset of superconductivity in ultrathin granular metal films, *Phys. Rev. B* **40**, 182 (1989).
- [27] Y. Liu, D. B. Haviland, B. Nease, and A. M. Goldman, Insulator-to-superconductor transition in ultrathin films, *Phys. Rev. B* **47**, 5931 (1993).
- [28] M. Thiemann, M. Dressel, and M. Scheffler, Complete electro-dynamics of a BCS superconductor with μeV energy scales: Microwave spectroscopy on titanium at mK temperatures, *Phys. Rev. B* **97**, 214516 (2018).
- [29] J. M. Graybeal and M. R. Beasley, Localization and interaction effects in ultrathin amorphous superconducting films, *Phys. Rev. B* **29**, 4167 (1984).
- [30] D. Shahar and Z. Ovadyahu, Superconductivity near the mobility edge, *Phys. Rev. B* **46**, 10917 (1992).
- [31] R. Matsunaga, N. Tsuji, H. Fujita, A. Sugioka, K. Makise, Y. Uzawa, H. Terai, Z. Wang, H. Aoki, and R. Shimano, Light-induced collective pseudospin precession resonating with Higgs mode in a superconductor, *Science* **345**, 1145 (2014).
- [32] R. Shimano and N. Tsuji, Higgs mode in superconductors, *Annu. Rev. Condens. Matter Phys.* **11**, 103 (2020).
- [33] U. S. Pracht, T. Cea, N. Bachar, G. Deutscher, E. Farber, M. Dressel, M. Scheffler, C. Castellani, A. M. García-García, and L. Benfatto, Optical signatures of the superconducting goldstone mode in granular aluminum: Experiments and theory, *Phys. Rev. B* **96**, 094514 (2017).
- [34] F. Levy-Bertrand, T. Klein, T. Grenet, O. Dupré, A. Benoît, A. Bideaud, O. Bourrion, M. Calvo, A. Catalano, A. Gomez, J. Goupy, L. Grünhaupt, U. v. Luepke, N. Maleeva, F. Valenti, I. M. Pop, and A. Monfardini, Electro-dynamics of granular aluminum from superconductor to insulator: Observation of collective superconducting modes, *Phys. Rev. B* **99**, 094506 (2019).
- [35] J. R. Schrieffer, *Theory of Superconductivity* (CRC Press, Boca Raton, FL, 2018).
- [36] See Supplemental Material at <http://link.aps.org/supplemental/10.1103/PhysRevB.105.094515> for further technical details about the calculation of full gauge-invariant current-current correlators and also includes results on both phase and amplitude spectral functions and the optical conductivity in the strong coupling limit.
- [37] M. Ma and P. A. Lee, Localized superconductors, *Phys. Rev. B* **32**, 5658 (1985).
- [38] A. Ghosal, M. Randeria, and N. Trivedi, Role of Spatial Amplitude Fluctuations in Highly Disordered s -Wave Superconductors, *Phys. Rev. Lett.* **81**, 3940 (1998).
- [39] A. Ghosal, M. Randeria, and N. Trivedi, Inhomogeneous pairing in highly disordered s -wave superconductors, *Phys. Rev. B* **65**, 014501 (2001).
- [40] J. Mayoh and A. M. García-García, Global critical temperature in disordered superconductors with weak multifractality, *Phys. Rev. B* **92**, 174526 (2015).
- [41] B. Fan and A. M. García-García, Enhanced phase-coherent multifractal two-dimensional superconductivity, *Phys. Rev. B* **101**, 104509 (2020).
- [42] B. Fan and A. M. García-García, Superconductivity at the three-dimensional Anderson metal-insulator transition, *Phys. Rev. B* **102**, 184507 (2020).
- [43] C. Rubio-Verdu, A. M. Garcia-Garcia, H. Ryu, D.-J. Choi, J. Zaldivar, S. Tang, B. Fan, Z.-X. Shen, S.-K. Mo, J. I. Pascual, and M. M. Ugeda, Visualization of multifractal superconductivity in a two-dimensional transition metal dichalcogenide in the weak-disorder regime, *Nano Lett.* **20**, 5111 (2020).
- [44] I. S. Burmistrov, I. V. Gornyi, and A. D. Mirlin, Enhancement of the Critical Temperature of Superconductors by Anderson Localization, *Phys. Rev. Lett.* **108**, 017002 (2012).
- [45] M. N. Gastiasoro and B. M. Andersen, Enhancing superconductivity by disorder, *Phys. Rev. B* **98**, 184510 (2018).
- [46] P. de Gennes, Boundary effects in superconductors, *Rev. Mod. Phys.* **36**, 225 (1964).
- [47] P. de Gennes, *Superconductivity of Metals and Alloys* (W. A. Benjamin, New York, 1966).